

Experiments with an isolated subatomic particle at rest

Hans Dehmelt

Department of Physics, University of Washington, Seattle, Washington 98195

You know, it would be sufficient to really understand the electron.

Albert Einstein

The 5th century B.C. Philosopher's Democritus' smallest conceivable in-divisible entity, the a-tomon (the uncuttable), is a most powerful, but not an immutable, concept. By 1930 it had already metamorphosed twice: from something similar to a molecule, say a slippery atom of water, to Mendeleev's chemist's atom and later to electron and to proton, both particles originally assumed to be of small but finite size. With the rise of Dirac's theory of the electron in the late twenties, their size shrunk to mathematically zero. Everybody "knew" then that electron and proton were indivisible Dirac point particles with radius $R=0$ and gyromagnetic ratio $g=2.00$. The first hint of cuttability or at least compositeness of the proton came from Stern's 1933 measurement of proton magnetism in a Stern-Gerlach molecular-beam apparatus. However, this was not realized at the time. He found for its normalized dimensionless gyromagnetic ratio not $g=2$ but

$$g = (\mu / A)(2M / q) \approx 5 ,$$

where μ , A , M , and q are, respectively, magnetic moment, angular momentum, mass, and charge of the particle. For comparison the obviously composite ${}^4\text{He}^+$ ion, also with spin $\frac{1}{2}$, according to the above formula has the $|g|$ value 14 700, much larger than the Dirac value 2. Also, along with this large $|g|$ value went a very finite radius of this atomic ion of about 3×10^{-11} m. And indeed, with Hofstadter's high-energy electron-scattering experiments in the fifties the proton radius grew again to $R = 0.86 \times 10^{-15}$ m roughly in proportion to the excess of 3 in g . Similar later work at still higher energies found three quarks inside the "indivisible" proton. Today everybody "knows" the *electron* is an indivisible atomon, a Dirac point particle with radius $R=0$ and $g=2.00$ But is it? Like the proton, it could be a composite object. History may well repeat itself. This puts a very high premium on precise measurements of the g factor of the electron.

GEONIUM SPECTROSCOPY

The metastable pseudo-atom geonium (Van Dyck *et al.*, 1978,1986) has been expressly synthesized for studies of the electron g factor under optimal conditions. It consists of an individual electron permanently confined in an ultrahigh vacuum Penning trap at 4 K. The trap

employs a homogeneous magnetic field $B_0=5$ T and a weak electric quadrupole field. The latter is produced by hyperbolic electrodes, a positive ring and two negative caps spaced $2Z_0=8$ mm apart, see Figure 1. The potential, with A a constant, is given by

$$\phi(xyz) = A(x^2 + y^2 - 2z^2) ,$$

with an axial potential-well depth

$$D = e[\phi(000) - \phi(00Z_0)] = 2eAZ_0^2 = 5 \text{ eV} .$$

The trapping is mostly magnetic. The large magnetic field dominates the motion in the geonium atom. The energy levels of this atom, shown in Fig. 2, reflect the cyclotron motion at frequency $\nu_c = eB_0/2\pi m = 141$ GHz, the spin precession at $\nu_s \approx \nu_c$, the anomaly or $g-2$ frequency $\nu_a = \nu_s - \nu_c = 164$ MHz, the axial oscillation at $\nu_z = 60$ MHz, and the magnetron or drift motion at frequency $\nu_m = 13$ kHz. The electron is continuously monitored by exciting the ν_z oscillation and detecting via radio the 10^8 -fold enhanced spontaneous 60 MHz emission. A corresponding signal appears in Figure 3. Doppler sideband cooling has made continuous confinement in the trap center of an electron for ten months (Gabrielse *et al.*, 1985) possible. This process makes the electron absorb rf photons deficient in energy and supply the balance from energy stored in the electron motion to be cooled. The corresponding shrinking of the radius of the magnetron motion is displayed in Figure 4. Extended into the optical region, the cooling scheme is most convincingly demonstrated in Figure 5. The transitions of primary in-

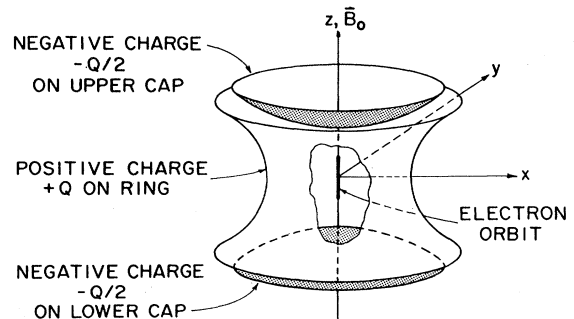


FIG. 1. Penning trap. The simplest motion of an electron in the trap is along its symmetry axis, along a magnetic-field line. Each time it comes too close to one of the negatively charged caps it turns around. The resulting harmonic oscillation took place at about 60 MHz in our trap. Reproduced from Dehmelt (1983) with permission, copyright Plenum Press.

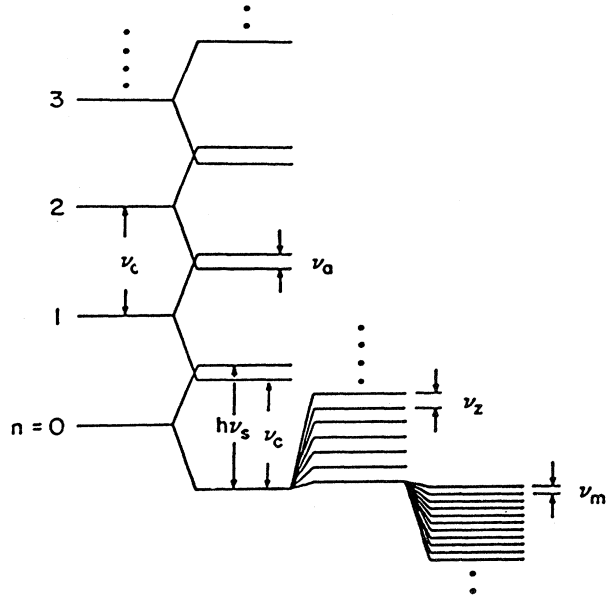


FIG. 2. Energy levels of geonium. Each of the cyclotron levels labeled n is split first by the spin-magnetic field interaction. The resulting sublevels are further split into the oscillator levels and finally the manifold of magnetron levels extending downwards. Reproduced from Van Dyck *et al.* (1978) with permission, copyright Plenum Press.

terest at ν_c, ν_a, ν_m are much more difficult to detect than the ν_z oscillation. Nevertheless the task may be accomplished by means of the continuous Stern-Gerlach effect (Dehmelt, 1988a), in which the geonium atom itself is made to work as a 10^8 -fold amplifier. In the scheme a single ν_a photon of only $\approx 1 \mu\text{eV}$ energy gates the absorption of $\approx 100 \text{ eV}$ of rf power at ν_z . The continuous effect uses an inhomogeneous magnetic field in a similar

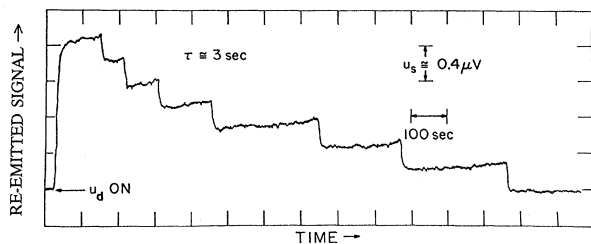


FIG. 3. rf signal produced by trapped electron. When the electron is driven by an axial rf field, it emits a 60 MHz signal, which was picked up by a radio receiver. The signal shown was for a very strong drive and an initially injected bunch of seven electrons. One electron after the other was randomly "boiled" out of the trap until finally only a single one is left. By somewhat reducing the drive power, this last electron could be observed indefinitely. Reproduced from Wineland *et al.* (1973) with permission, copyright American Institute of Physics.

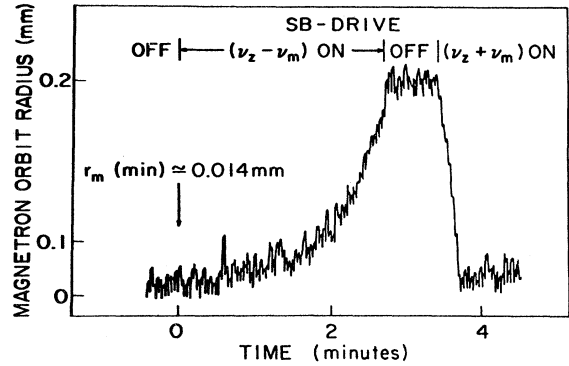


FIG. 4. Sideband "cooling" of the magnetron motion at ν_m . By driving the axial motion not on resonance at ν_z but on the lower Doppler sideband at $\nu_z - \nu_m$, it is possible to force the metastable magnetron motion to provide the energy balance $h\nu_m$, and thereby expand the magnetron orbit radius. Conversely, an axial drive at $\nu_z + \nu_m$ shrinks the radius. The roles of upper and lower sidebands are reversed here from the case of a particle in a well where the energy increases with amplitude because the magnetron motion is metastable and the total energy of this motion *decreases* with radius. Reproduced from Van Dyck *et al.* (1978) with permission, copyright Plenum Press.

way as the classic one. However, the field takes now the form of a very weak Lawrence cyclotron trap or magnetic bottle, shown in Figure 6. The bottle adds a minute monitoring well only

$$D_m = (m + n + \frac{1}{2})0.1 \mu\text{eV}$$

deep to the axial well of large electrostatic depth $D=5 \text{ eV}$, with m, n , respectively, denoting spin and cyclotron quantum numbers. Thus jumps in m or n show up as jumps in ν_z ,

$$\nu_z = \nu_{z0} + (m + n + \frac{1}{2})\delta,$$

with $\delta=1.2 \text{ Hz}$ in our experiments, and ν_{z0} the axial frequency of the electron without a magnetic bottle. Random jumps in m, n occur when spin or cyclotron resonances are excited. Figure 6(a) shows an early example of a series of such jumps in m or spin flips. For the spin spontaneous transitions are totally negligible. Standard text books discuss transitions between two sharp levels induced by a broad electromagnetic spectrum $\rho(\nu)$: The transition rate from either level is the same and is proportional to the spectral power density $\rho(\nu_s)$ of the radiation field at the transition frequency ν_s . Ergo, the average dwell times in either level are the same, compared Figure 6(a). In the geonium experiments the frequency of the weak rf field is sharp, but the spin resonance is broadened and has a shape $G_s(\nu)$. One may convince oneself that moving the sharp frequency of the rf field upwards over the broad spin resonance should produce the same results as moving a broad rf field of spectral shape $\rho(\nu) \propto G_s(\nu)$ downwards over a sharp spin resonance:



FIG. 5. Visible blue (charged) barium atom Astrid at rest in center of Paul trap photographed in natural color. The photograph strikingly demonstrates the close localization, $\ll 1 \mu\text{m}$, attainable with geonium cooling techniques. Stray light from the lasers focused on the ion also illuminates the ring electrode of the tiny rf trap of about 1 mm internal diameter. Reproduced from Dehmelt (1988) with permission, copyright the Royal Swedish Academy of Sciences.

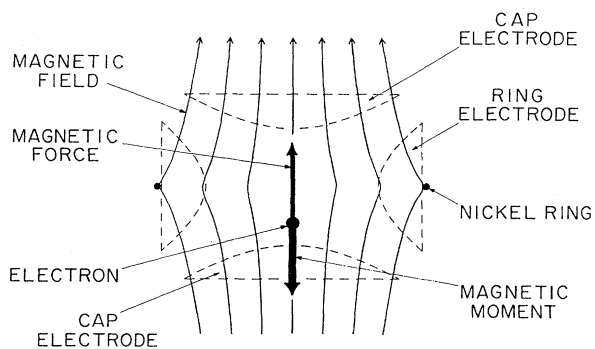


FIG. 6 Weak magnetic bottle for continuous Stern-Gerlach effect. When in the lowest cyclotron and magnetron level, the electron forms a $1 \mu\text{m}$ long wave packet, 30 nm in diameter, which may oscillate undistorted in the axial electric potential well. The inhomogeneous field of the auxiliary magnetic bottle produces a minute spin-dependent restoring force that causes the axial frequency ν_z for spin \uparrow and \downarrow to differ by a small but detectable value. Reproduced from Dehmelt (1988a) with permission, copyright Springer-Verlag.

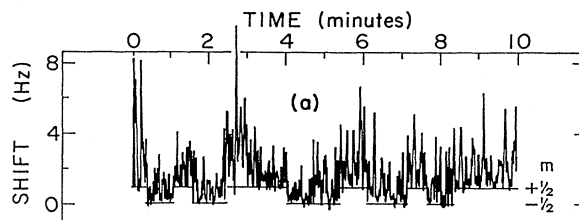


FIG. 6(a). Spin flips recorded by means of the continuous Stern-Gerlach effect. The random jumps in the base line indicate jumps in m at a rate of about 1/minute when the spin resonance is excited. The upwards spikes or "cyclotron grass" are explained by expected rapid random thermal excitation and spontaneous decay of cyclotron levels with an average value $\langle n \rangle \approx 1.2$. Adapted from Van Dyck *et al.* (1977) with permission, copyright American Institute of Physics.

The rate of all spin flips or jumps in m in either direction counted in the experiment is proportional to $G_s(\nu)$. To obtain the plot of $G_s(\nu)$ in Figure 7, the frequency of the rf field was increased in small steps, and at each step spin flips were counted for a fixed period of about $\frac{1}{2}$ hour. From our ν_s, ν_c data for electron and positron (Van Dyck *et al.*, 1987), we have determined

$$\frac{1}{2}g^{\text{exp}} = \nu_s / \nu_c = 1.001\,159\,652\,188(4),$$

the same for particle and antiparticle. The error in the difference of their g factors is only half as large. Heroic quantum electro-dynamical calculations (Kinoshita, 1988) have now yielded for the shift of the g factor of a point electron associated with turning on its interaction with the electromagnetic radiation field

$$\begin{aligned} \frac{1}{2}(g^{\text{point}} - 2) &= \frac{1}{2}\Delta g^{\text{Kinoshita}} \\ &= 0.001\,159\,652\,133(29). \end{aligned}$$

In the calculations $\Delta g^{\text{Kinoshita}}$ is expressed as a power series in α/π . Kinoshita has critically evaluated the experimental α input data on which he must rely. He warns that the error in his above result, which is dominated by the error in α , may be underestimated. Muonic, hadronic, and other small contributions to g amount to less than about 4×10^{-12} and have been included in the shift. Kinoshita's result may be used to correct the experimental g value and find

$$g = g^{\text{exp}} - \Delta g^{\text{Kinoshita}} = 2 + 11(6) \times 10^{-11}.$$

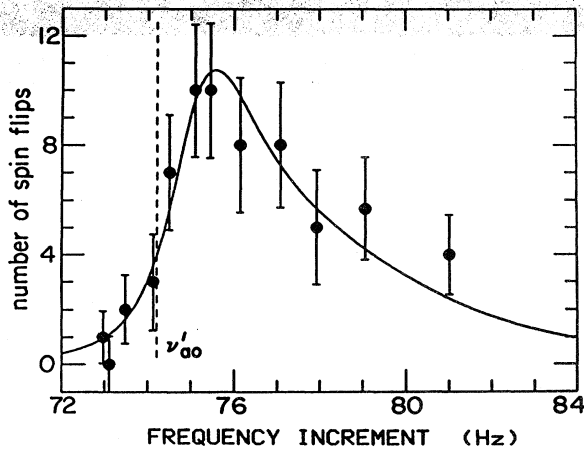


FIG. 7. Plot of electron spin resonance in geonium near 141 GHz. A magnetic radio-frequency field causes random jumps in the spin quantum number. As the frequency of the exciting field is stepped through the resonance in small increments, the number of spin flips occurring in a fixed observation period of about $\frac{1}{2}$ hour are counted and then plotted vs frequency. (Actually the 141 GHz field flipping the spin is produced by the cyclotron motion of the electron through an inhomogeneous magnetic rf field at $\nu_s - \nu_c = 164$ MHz.) Reproduced from Van Dyck *et al.* (1987) with permission, copyright American Institute of Physics.

ELECTRON RADIUS R ?

Extrapolation from known to unknown phenomena is a time-honored approach in all the sciences. Thus from known g , and R values of other near-Dirac particles and our measured g value of the electron, I attempt to extrapolate a value for its radius. Stimulated by 1980 theoretical work of Brodsky and Drell, I (1989a) have plotted $|g - 2|$ vs R/λ_c in Figure 8 for the helium-3 nucleus, triton, proton, and electron. Here λ_c is the Compton wavelength of the respective particle. The plausible relation given by Brodsky and Drell (1980) for the simplest composite theoretical model of the electron,

$$|g - 2| = R / \lambda_c,$$

or

$$|g - g_{\text{Dirac}}| = (R - R_{\text{Dirac}}) / \lambda_c,$$

fits the admittedly sparse data surprisingly well. Even for such a very different spin $\frac{1}{2}$ structure as the atomic ion ${}^4\text{He}^+$ composed of an α particle and an electron, the data

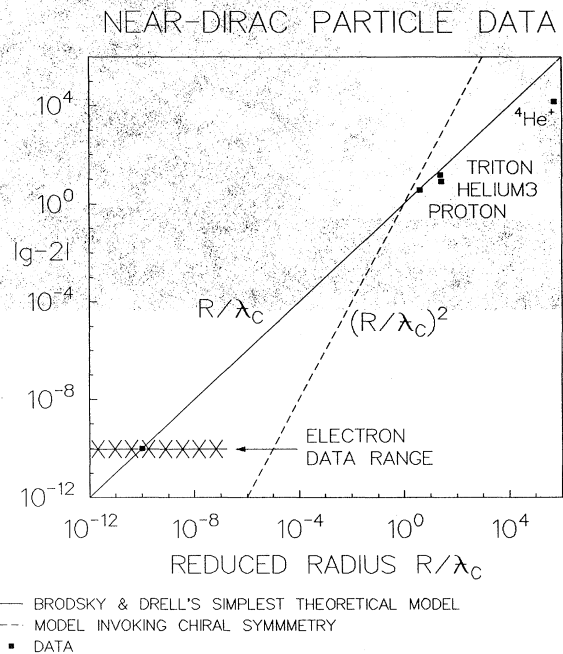


FIG. 8. Plot of $|g - 2|$ values, with radiative shifts removed, vs reduced rms radius R/λ_c for near-Dirac particles. The full line $|g - 2| = R/\lambda_c$ predicted by the simplest theoretical model provides a surprisingly good fit to the data for proton, triton, and helium-3 nucleus. It may be used to obtain a new radius value for the *physical* electron from its intersection with the line $|g - 2| = 1.1 \times 10^{-10}$ representing the Seattle electron g data. The data are much less well fitted by the relation $|g - 2| = (R/\lambda_c)^2$, which is shown for comparison in the dashed line. The atomic ion ${}^4\text{He}^+$ is definitely *not* a near-Dirac particle, but even its data point does not fall too far off the full line. Adapted from Dehmelt (1990) with permission, copyright American Institute of Physics.

point does not fall too far off the full line. Intersection in Figure 8 of this line with the line $|g - 2| = 1.1 \times 10^{-10}$ for the Seattle g data yields for the electron the extrapolated point shown and with $\lambda_c = 0.39 \times 10^{-10}$ cm an electron radius

$$R \approx 10^{-20} \text{ cm} .$$

The row of \times 's reflects the data range defined by the uncertainty in the Seattle g data and the upper limit $R < 10^{-17}$ cm determined in high-energy collision experiments. It appears that this combination of current data is not in harmony with electron structure models assuming special symmetries that predict the quadratic relation $|g - 2| \approx (R/\lambda)^2$ shown by the dashed line. This favors the linear relation used in the above extrapolation of R for the electron. Thus the electron may have *size and structure!*

If one feels that the excess g value $11(6) \times 10^{-11}$ measured is not significant because of its large relative error, then the value $R \approx 10^{-20}$ cm given here still constitutes an important new upper limit. Changing the point of view, the close agreement of g^{point} with g^{exp} provides the most stringent experimental test of the fundamental theory of Quantum Electrodynamics in which $R=0$ is assumed. Furthermore the near-identity of the g values measured for electron and positron in Seattle constitutes the most severe test of the CPT theorem or mirror symmetry of a *charged* particle pair.

LEMAÎTRE'S "L'ATOME PRIMITIF" REVISITED—A SPECULATION

Beginning 1974 Salam and others have proposed composite electron and quark models (Lyons, 1983). On the strength of these proposals and with an eye on Figure 8, I view the electron as the third approximation of a Dirac particle, d_3 for short, and as composed of three fourth-approximation Dirac or d_4 particles. The situation is taken to be quite similar to that previously encountered in the triton and proton subatomic particles, respectively, assumed to be of type d_1 and d_2 . In more detail, three d_4 subquarks of huge mass $m' \approx 10^{10} m_e$ in a deep square well make up the electron in this working hypothesis. However, their mass $3m'$ is almost completely compensated by strong binding to yield a total relativistic mass equal to the observed mass m_e of the electron. Figure 8 may even suggest a more speculative extrapolation: The e constituents, in the infinite regression $N \rightarrow \infty$ proposed in Figure 9, have ever more massive, ever smaller sub-sub-... constituents d_N . However, these higher-order subquarks are realized only up to the "cosmon" with $N=C$, the most massive particle ever to appear in this universe.* At the beginning of the universe, a lone

*A single "monotheistic" entity terminating a *finite* sequence of preons, pre-preons, pre-pre-preons... has been briefly discussed in *Preon Model*, by J. C. Pati, A. Salam, and J. Strathdee, Nucl. Phys. **B185**, 416 (1981).

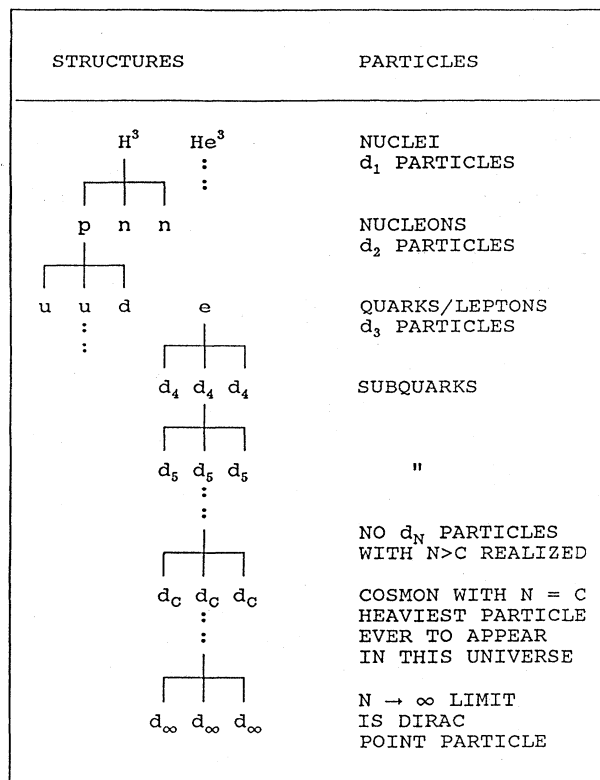


FIG. 9. Triton model of near-Dirac particles. Reproduced from Dehmelt (1989b) with permission, copyright the National Academy of Sciences of the USA.

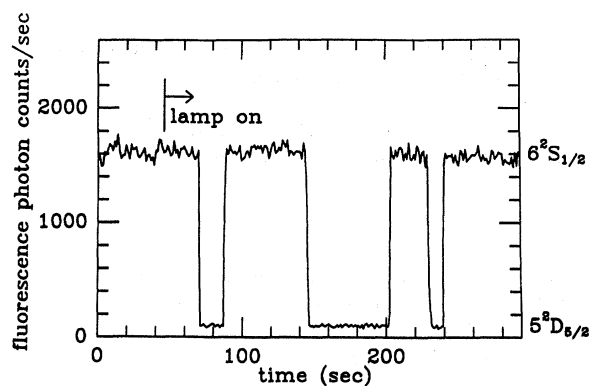


FIG. 10. Spontaneous decay of Ba^+ ion in metastable $D_{5/2}$ -level. Illuminating the ion with a laser tuned close to its resonance line produces strong resonance fluorescence and an easily detectable photon count of 1600 photons/sec. When later an auxiliary, weak Ba^+ spectral lamp is turned on, the ion is randomly transported into the metastable $D_{5/2}$ level of 30 sec lifetime and becomes invisible. After dwelling in this shelving level for 30 sec on the average, it drops down to the $S_{1/2}$ ground state spontaneously and becomes visible again. This cycle then repeats. Reproduced from Nagourney *et al.* (1986) with permission, copyright American Institute of Physics.

bound cosmon-anticosmon pair or life time-broadened cosmonium atom state of near-zero total relativistic mass/energy was created from Vilenkin's (1984) metastable "nothing" state of zero relativistic energy in a spontaneous quantum jump of cosmic rarity. Similar, though much more frequent, quantum jumps that have recently been observed in a trapped Ba^+ ion are shown in Figure 10. In this case the system also jumps spontaneously from a state (ion in metastable $D_{5/2}$ level plus no photon) to a new state (ion in $S_{1/2}$ ground level plus photon) of the same total energy. The "cosmonium atom" introduced here is merely a modernized version[†] of Lemaître's "l'atome primitif" or world-atom whose explosive radioactive decay created the universe. At the beginning of the world the short-lived cosmonium atom decayed into an early gravitation-dominated standard big-bang state that eventually developed into a state, in which again rest mass energy, kinetic, and gravitational potential energy add up to *zero* (see formula 8 of Jordan, 1937). The electron is a much more complex particle than the cosmon. It is composed of 3^{C-3} cosmon-like d_C 's, but only two particles of this type formed the cosmonium world-atom from which sprang the universe. In closing, I should like to cite a line from *William Blake*,

"To see a world in a grain of sand--"

and allude to a possible parallel

--to see worlds in an electron--

REFERENCES

- Brodsky, S. J., and S. D. Drell (1980), "Anomalous Magnetic Moment and Limits on Fermion Substructure," *Phys. Rev. D* **22**, 2236.
- Dehmelt, H. (1983), "Stored Ion Spectroscopy," in *Advances in Laser Spectroscopy*, edited by F. T. Arecchi, F. Strumia, and H. Walther (Plenum, New York).
- Dehmelt, H. (1988a), "Single Atomic Particle Forever Floating at Rest in Free Space: New Value for Electron Radius," *Phys. Scr.* **T22**, 102.
- Dehmelt, H. (1988b), "New Continuous Stern Gerlach Effect and a Hint of 'the' Elementary Particle," *Z. Phys. D* **10**, 127-134.
- Dehmelt, H. (1989a), "Geonium Spectra*Electron Radius *Cosmon," in *High Energy Spin Physics*, 8th International Symposium, edited by K. Heller (AIP Conf. Proc. No. 187) (AIP, New York), p. 319.
- Dehmelt, H. (1989b), "Triton. . .electron. . .cosmon. . .: An infinite regression?" *Proc. Natl. Acad. Sci. USA* **86**, 8618-8619.
- Dehmelt, H. (1990), "Less is more: Experiments with an Individual Atomic Particle at Rest in Free Space," *Am. J. Phys.* **58**, 17.
- Gabrielse, G., H. Dehmelt, and W. Kells (1985), "Observation of a Relativistic, Bistable Hysteresis in the Cyclotron Motion of a Single Electron," *Phys. Rev. Lett.* **54**, 537.
- Jordan, P. (1937), "Die physikalischen Weltkonstanten," *Naturwissenschaften* **25**, 513.
- Kinoshita, T. (1988), "Fine-Structure Constant Derived from Quantum Electrodynamics," *Metrologia* **25**, 233.
- Lemaître, G. (1950), *The Primeval Atom* (Van Nostrand, New York), p. 77.
- Lyons, L. (1983), "An Introduction to the Possible Substructure of Quarks and Leptons," *Prog. Part. Nucl. Phys.* **10**, 227; see references cited herein.
- Nagourey, W., J. Sandberg, and H. Dehmelt (1986), "Shelved Optical Electron Amplifier: Observation of Quantum Jumps," *Phys. Rev. Lett.* **56**, 2797.
- Van Dyck, R. S., Jr., P. Ekstrom, and H. Dehmelt (1977), "Precise Measurement of Axial, Magnetron, and Spin-Cyclotron Beat Frequencies on an Isolated 1-meV Electron," *Phys. Rev. Lett.* **38**, 310.
- Van Dyck, R. S., Jr., P. B. Schwinberg, and H. G. Dehmelt (1978), "Electron Magnetic Moment from Geonium Spectra," in *New Frontiers in High Energy Physics*, edited by B. Kursumoglu, A. Perlmutter, and L. Scott (Plenum, New York).
- Van Dyck, R. S., Jr., P. B. Schwinberg, and H. G. Dehmelt (1986), "Electron Magnetic Moment from Geonium Spectra: Early Experiments and Background Concepts," *Phys. Rev. D* **34**, 722.
- Van Dyck, R. S., Jr., P. B. Schwinberg, and H. G. Dehmelt (1987), "New High Precision Comparison of Electron/Positron g-Factors," *Phys. Rev. Lett.* **59**, 26.
- Vilenkin, A. (1984), "Quantum Creation of Universe," *Phys. Rev. D* **30**, 509-515.
- Wineland, D., P. Ekstrom, and H. Dehmelt (1973), "Monoelectron Oscillator," *Phys. Rev. Lett.* **31**, 1297.

[†]This is by no means the first modernization attempt. M. Goldhaber has kindly brought it to my attention that he had introduced a different "cosmon" already in 1956 in his paper "Speculations on Cosmogony," *Science* **124**, 218.

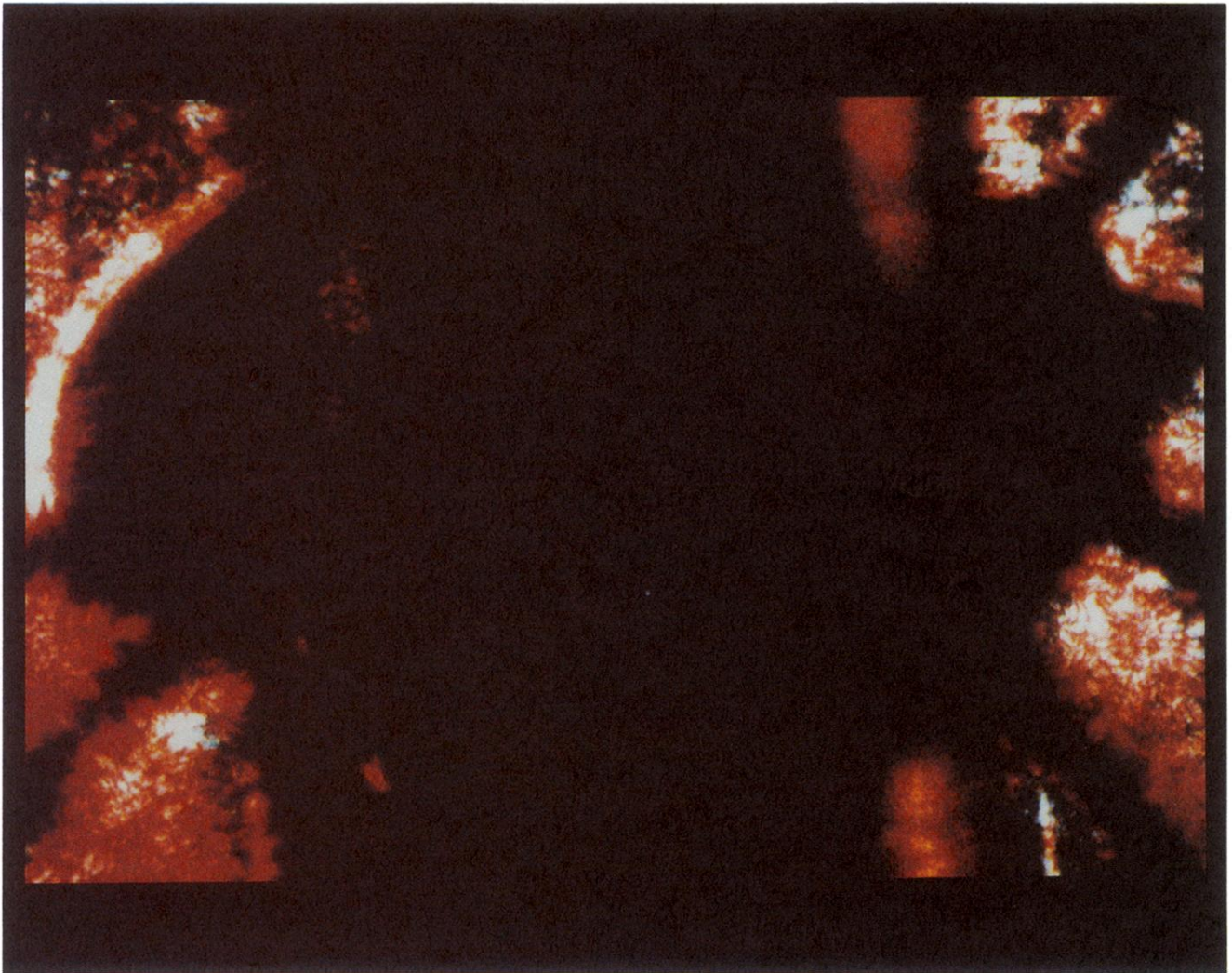


FIG. 5. Visible blue (charged) barium atom Astrid at rest in center of Paul trap photographed in natural color. The photograph strikingly demonstrates the close localization, $\ll 1 \mu\text{m}$, attainable with geonium cooling techniques. Stray light from the lasers focused on the ion also illuminates the ring electrode of the tiny rf trap of about 1 mm internal diameter. Reproduced from Dehmelt (1988) with permission, copyright the Royal Swedish Academy of Sciences.